


Wave-number selection in pattern-forming systemsS. Saxena  and J. M. Kosterlitz*Department of Physics, Brown University, Providence, Rhode Island 02912, USA*

(Received 8 February 2019; published 28 August 2019)

Wave-number selection in pattern-forming systems remains a long-standing puzzle in physics. Previous studies have shown that external noise is a possible mechanism for wave-number selection. We conduct an extensive numerical study of the noisy stabilized Kuramoto-Sivashinsky equation. We use a fast spectral method of integration, which enables us to investigate long-time behavior for large system sizes that could not be investigated by earlier work. We find that a state with a unique wave number has the highest probability of occurring at very long times. We also find that this state is independent of the strength of the noise and initial conditions, thus making a convincing case for the role of noise as a mechanism of state selection.

DOI: [10.1103/PhysRevE.100.022223](https://doi.org/10.1103/PhysRevE.100.022223)**I. INTRODUCTION**

This work addresses the question of wave-number selection in pattern-forming systems. Pattern-forming systems are characterized by the emergence of a band of spatially periodic steady states, as a certain quantity called the control parameter is varied [1]. Examples of pattern-forming systems in physics are Rayleigh-Bénard convection [1] and directional solidification [2]. Although a large number of periodicities are mathematically allowed in such systems, experiments and simulations of realistic physical systems have repeatedly shown that only a narrow range of periodicities is realized in practice. The tendency of a system to prefer a narrow set of states out of many possible states is known as wave-number selection.

Many mechanisms have been proposed to explain this phenomenon. These include evolution from random initial conditions having a power spectrum centered at a given wave number [3,4] and control parameter ramps [5–7] (see Sec. III for a brief discussion). Various computational studies [8–11] have also investigated the role of additive stochastic noise in wave-number selection. The idea that noise can trigger wave-number selection can be justified with the help of a simple dynamical system which evolves in a relaxational manner; i.e., it minimizes a potential energy. If the potential has several local minima, the deterministic system will evolve to one of these minima, depending on the initial conditions. However, in the presence of noise, the system will escape from any local minima and eventually reach the global minimum of the potential energy, where it will then spend most of its time, provided the noise strength is small. This has been investigated in Ref. [12] for the Swift-Hohenberg model [13], which is a potential system. While this example of a potential system illustrates wave-number selection, the systems that are described in Refs. [8–11] do *not* have a potential energy function. The role of noise in inducing wave-number selection in nonpotential systems is not well understood.

In this paper, we further explore the role of noise as a mechanism for wave-number selection in a model known as the stabilized Kuramoto-Sivashinsky (SKS) equation [14]. There are two main reasons for this choice. First, we chose

this model because it exhibits rich nonlinear behavior and a band of spatially periodic stationary states, while being relatively simple and one-dimensional, which makes simulating it easy. The second reason is that it is nonvariational, i.e., the deterministic driving force cannot be expressed as the gradient of a potential. Thus, we expect that studying this system would shed light on wave-number selection in systems where minimization of a potential cannot explain selection of a particular state.

Noise-induced wave-number selection in this model has been studied before using direct numerical simulation [11], but only for small systems and a limited range of control parameters. More recently, Qiao *et al.* [15] used path integral methods to find the selected wave number for a range of control parameter values. It is of considerable interest to extend the work in Ref. [11] to larger system sizes, because numerical simulation of any periodic problem necessarily allows only a discrete set of wave numbers, and these discrete wave numbers are widely separated for small system sizes. Thus, the uncertainty in the selected wave number obtained for a small system is large. Therefore, our aim in this work is to obtain more precise estimates for the selected wave number by simulating larger systems and to cover a wider range of control parameter values. We also wish to determine if the results of Ref. [15] can be reproduced through direct integration.

This paper is organized as follows: Sec. II introduces the mathematical formalism used to study pattern-forming systems and describes the SKS model. Section III describes in detail the results of Refs. [11] and [15]. Section IV describes our computational method, and Sec. V shows some of our results and their interpretation. Finally, Sec. VI discusses some of the drawbacks of our computational methods and touches on potential improvements that will be the focus of future work.

II. PATTERN FORMATION AND THE SKS MODEL

Pattern-forming systems such as the ones mentioned above are represented by nonlinear partial differential equations that

govern the evolution of a given physical quantity. In general, the equation for such a system is of the form

$$\partial_t u(x, t) = \hat{\mathbf{L}}_p u(x, t) + \hat{\mathbf{N}}[u(x, t)], \quad (1)$$

where $u(x, t)$ is a field representing the quantity of interest, $\hat{\mathbf{L}}_p$ is a linear differential operator acting on $u(x, t)$, and $\hat{\mathbf{N}}[u(x, t)]$ is a nonlinear operator. The subscript p on the linear operator indicates that it depends on the control parameter p . As an example, in the case of directional solidification, the quantity of interest $u(x, t)$ is the position of the interface between the liquid and solid phases. The trivial solution (or base state) $u_b(x, t) = 0$ is generally a stationary state of these equations. However, this solution is stable only for a certain range of values of p . After p crosses a critical value p_c , the trivial, spatially uniform state becomes unstable to periodic perturbations, and a band of stable, periodic steady states emerges. To determine when the uniform state becomes unstable, we imagine adding to the uniform base state $u_b(x, t) = 0$ the perturbation $\delta u \sim e^{iqx + \sigma(q)t}$. This perturbation is periodic in space with wave number q and grows with time at a rate σ . We then substitute $u(x, t) = u_b(x, t) + \delta u$ in Eq. (1), retain only terms linear in δu , and derive an expression for the growth rate σ as a function of q . If, for a given value of p , $\text{Re}[\sigma(q)]$ is negative, that means that the perturbations with those wave numbers decay exponentially with time, and hence the uniform base state u_b is stable to those perturbations. However, if $\text{Re}[\sigma(q)]$ is positive, then perturbations with wave number q grow exponentially with time, implying that the base state is unstable to them. Of course, in practice, the unbounded exponential growth of these perturbations is balanced by the nonlinear terms in the original equation.

To make these ideas more concrete, we illustrate the above steps for the deterministic SKS model. The SKS equation is given by

$$\partial_t u(x, t) = -\alpha u(x, t) - \partial_x^2 u(x, t) - \partial_x^4 u(x, t) + [\partial_x u(x, t)]^2. \quad (2)$$

Here α plays the role of the control parameter, and $u(x, t)$ is a dimensionless field of dimensionless space-time variables. This equation is used to describe directional solidification [14] and the Burton-Cabrera-Frank model of terrace growth [16]. The trivial solution $u_b(x, t) = 0$ is one of the steady states of this equation. We now add to this solution a small perturbation of the form $\delta u \sim e^{iqx + \sigma(q)t}$. Substituting into Eq. (2) and linearizing about the base state ($u_b(x, t) = 0$) give us an expression for the growth rate:

$$\sigma = -\alpha + q^2 - q^4. \quad (3)$$

From this, we see that the growth rate is real and non-negative for $1/2 - \sqrt{1/4 - \alpha} \leq q^2 \leq 1/2 + \sqrt{1/4 - \alpha}$ and $\alpha \leq 1/4$, as shown in Fig. 1. We do not consider imaginary solutions of Eq. (3) here, which correspond to oscillatory instabilities. For values of q in the above range, the state $u_b(x, t) = 0$ is unstable. By solving the equation $\frac{\partial \sigma}{\partial q} = 0$, we see that the growth rate is maximum for $q = q_c = 1/\sqrt{2}$, for all α . In summary, for $\alpha \leq 1/4 = \alpha_c$, a band of periodic steady states exists, with wave numbers given by

$$1/2 - \sqrt{1/4 - \alpha} \leq q^2 \leq 1/2 + \sqrt{1/4 - \alpha}, \quad \alpha \leq \alpha_c. \quad (4)$$

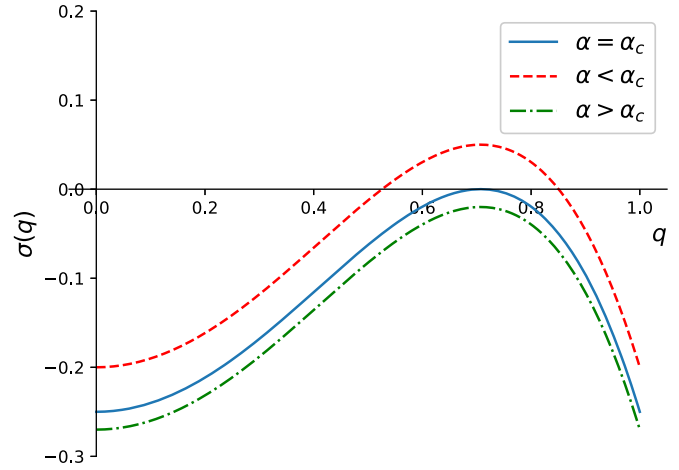


FIG. 1. Growth rate of periodic modes for values of α below, above, and at the threshold value $\alpha_c = 0.25$.

These periodic states may themselves be unstable to long wavelength periodic perturbations. Hence, in practice, one observes a band of periodic states that is narrower than suggested by Eq. (4) and is called the Eckhaus stable band [3]. Wave numbers within this band are stable to long wavelength periodic perturbations.

III. PREVIOUS STUDIES OF WAVE-NUMBER SELECTION

As mentioned in the Introduction, many possible explanations for wave-number selection have been suggested. Schober *et al.* [4] studied wave-number selection in the context of the one-dimensional Swift-Hohenberg equation [13]. The deterministic equation was integrated numerically, starting from random initial conditions with a power spectrum centered at a particular wave number \bar{k} . It was observed that the width of the noise-averaged power spectrum (or the structure function) decreased with time until a sharp power spectrum centered about a final wave number k_∞ was obtained. Their simulations showed that the final wave number depended on the value of \bar{k} .

Another proposed mechanism is the slow spatial variation of the control parameter, so that it changes from a value below the threshold in one part of the experimental apparatus to a value above the threshold in another part of the apparatus. This has been investigated experimentally [5] for the case of rotating Couette-Taylor flow. The experimental apparatus consists of two coaxial cylinders, separated by a gap that contains fluid. The inner cylinder is allowed to rotate with a given angular velocity. The control parameter, which is a function of the gap, is varied gradually by reducing the gap linearly towards the bottom of the apparatus. The variation in the gap is characterized by the angle made by the outer wall with the vertical. The wavelength of the resulting flow pattern was measured in the straight section for different bulk values of the control parameter and was observed to lie in a narrow band, whose width decreased as the control parameter was increased beyond the threshold. The observed wavelength was also found to be a periodic function of the aspect ratio (the ratio of the length of the straight section to the gap). The

role of ramps has also been studied analytically [6,7]. Ramps provide an efficient way to obtain a desired, well-defined periodic state. However, it must be noted that Ref. [7] shows that varying different quantities which influence the control parameter leads to different selected wave numbers. This implies that the selected wave number depends either on the initial conditions or, in the case of control parameter ramps, on the chosen ramping protocol. In other words, the selected wave number in a deterministic system is not an intrinsic property of the system itself, but depends on the measuring protocol.

The role of noise in inducing wave-number selection is the subject of some debate. While thermal noise is small enough that its effect on macroscopic patterns can be neglected [1], the same cannot be said about noise in an experimental apparatus [8–11,17,18]. As argued in Ref. [9], it is hard to precisely control experimental conditions in situations such as directional solidification, leading to uncertainties which are most easily modeled as additive noise. Studies have also shown that *multiplicative* noise can have nontrivial consequences on the dynamics of bifurcations, such as shifting the primary bifurcation point in the Swift-Hohenberg equation [17] and inducing new patterns which are absent in the deterministic system [18]. In addition, Refs. [8–11] have shown evidence of additive noise-induced wave-number selection. In our view, the other mechanisms mentioned above are too deterministic because they sample only a restricted set of perturbations. In contrast, stochastic noise is the most unbiased mechanism possible because it perturbs all periodic states of the deterministic system equally and does not favor a particular wave number over the others. It also samples a much larger set of perturbations. Hence, it is our view that more work needs to be done to gain a deeper understanding of the effects of noise, whether additive or multiplicative.

A notable study on noise-induced wave-number selection was performed by Kurtze [19]. This work used a WKB approximation [20] to estimate the stationary probability distribution for a general stochastic differential equation. The selected wave number was determined to be the one that maximized the stationary probability distribution. This method was applied to the Greenside-Cross equation [21] in one dimension and was found to give good agreement with direct numerical simulations. However, to our knowledge, Kurtze's method has, so far, not been used to find the selected wave number for other pattern-forming systems. A study by Hernández-García *et al.* [22,23] found that for the Swift-Hohenberg equation, the presence of noise smears the boundaries of the Eckhaus band, resulting in a smooth transition region between stable and unstable wave numbers. It was also found that the time evolution of the dominant wave number obeyed a scaling form.

For the particular case of the SKS equation, Obeid *et al.* [11] and Qiao *et al.* [15] have recently investigated noise-induced wave-number selection. We present here a brief summary of their results, which are relevant to this work. Obeid *et al.* carried out direct numerical simulations of the noisy SKS equation

$$\partial_t u(x, t) = -\alpha u - \partial_x^2 u(x, t) - \partial_x^4 u(x, t) + [\partial_x u(x, t)]^2 + \zeta(x, t), \quad (5)$$

where $\zeta(x, t)$ is an additive Gaussian noise satisfying

$$\langle \zeta(x, t) \rangle = 0 \quad (6)$$

and

$$\langle \zeta(x, t) \zeta(x', t') \rangle = 2\varepsilon \delta(x - x') \delta(t - t'). \quad (7)$$

Here ε is the noise strength. Equation (5) was discretized using a simple finite difference scheme, and the time integration was performed using the explicit forward Euler method. Various values of α between 0.17 and 0.24 and noise strengths ranging from 10^{-5} to 10^{-3} were studied. For $\alpha = 0.24$, it was found that the state with $q = 0.6995$ was most stable, in the sense that the system could not be knocked out of this state for 10^8 time steps, with noise strengths up to $\varepsilon = 5 \times 10^{-4}$.

For α values farther from the critical value of 0.25, no unique state could be identified as being most stable. For $\alpha = 0.2$, the allowed wave numbers are $0.589 \leq q \leq 0.767$. It was found that states with $0.650 \leq q \leq 0.712$ all remained stable up to 10^8 time steps and noise strengths up to $\varepsilon = 2 \times 10^{-3}$. Similarly, for $\alpha = 0.17$, states with $0.650 \leq q \leq 0.699$ were found to remain stable at 10^8 time steps and noise strengths up to $\varepsilon = 2 \times 10^{-3}$. It was therefore concluded that very long computational times would be required to destroy the stability of the states. In summary, the simulations in Ref. [11] hinted that the noise does indeed select a narrow band of wave numbers over others. However, selection of a unique state could be demonstrated only for $\alpha = 0.24$. A conclusive numerical demonstration of state selection therefore requires integration over large system sizes (to reduce discretization errors), long times, and a wider range of control parameters.

A more recent study of state selection in the SKS equation was conducted by Qiao *et al.* [15]. They used the least action principle of Freidlin-Wentzell theory [24] to calculate transition probabilities between pairs of periodic steady states for the SKS equation. For the stochastic process defined on a spatial domain $[0, L]$

$$\dot{\Phi}(x, t) = f[\Phi(x, t)] + \zeta(x, t), \quad (8)$$

the probability of a particular trajectory $\Phi(x, t) = \phi(x, t)$ defined over a time interval $[0, T]$ is

$$P_T[\phi(x, t)] = \mathcal{N} \exp\{-S_T[\phi(x, t)]/\varepsilon\}, \quad (9)$$

where \mathcal{N} is a normalization constant independent of $\phi(x, t)$, ε is the noise strength defined by

$$\langle \zeta(x, t) \zeta(x', t') \rangle = 2\varepsilon \delta(x - x') \delta(t - t'), \quad (10)$$

and $S_T[\phi(x, t)]$ is the action, given by

$$S_T[\phi(x, t)] = \frac{1}{2} \int_0^T dt \int_0^L dx \{\dot{\phi}(x, t) - f[\phi(x, t)]\}^2. \quad (11)$$

Equation (9) implies that the most probable trajectory connecting two states of the system is the one which minimizes the action. The most likely paths entering and leaving successive periodic states of the SKS equation were computed by finding the minimum action for transitions between those states (for example, $S_{q_j \rightarrow q_{j+1}}^*$ is the minimum action to go from a periodic state with wave number q_j to one with wave number q_{j+1} , and $S_{q_{j+1} \rightarrow q_j}^*$ is the minimum action for the reverse transition). These values were then used to determine

the net direction of transitions between two adjacent states. By implementing this procedure for all pairs of successive steady states, the wave number corresponding to the selected state was found. In order to minimize the actions $S_{q_j \rightarrow q_{j+1}}$ and $S_{q_{j+1} \rightarrow q_j}$, the saddle state between the states q_j and q_{j+1} was found numerically. The saddle state of the lowest order amplitude equation [1,25] was used as the initial guess for this procedure. Having found the saddle state, the time-reversed deterministic paths between the saddle state and the states q_j and q_{j+1} were used as initial guesses to find the minimum action paths (see Sec. III B of Ref. [15] for a detailed discussion).

IV. CALCULATING THE EMPIRICAL PROBABILITY DISTRIBUTION OF FINAL STATES

Although Qiao *et al.* have devised a way to calculate the selected wave number for the SKS problem, we wish to know if the same results can be obtained by direct integration of the equation of motion. There are two hurdles that must be overcome in order to do so. The first is that farther from the threshold, several neighboring states in the middle of the Eckhaus band become very stable to noise [11]. In order to determine which one, if any, is the most stable, one has to induce transitions between these states, so that the state in which the system spends most of its time is the most stable state. Observing such transitions between highly stable states requires extremely long integration times, as noted in Ref. [11]. The second hurdle is that simulations must be performed on very large systems due to the reasons mentioned in the Introduction. These two hurdles suggest that one look for a fast and efficient integration algorithm. Here we used a semi-implicit, Fourier spectral integration method [26]. Using a semi-implicit time integration scheme instead of explicit time integration allows one to use a significantly larger time step without compromising on accuracy, thus yielding a much higher speed of integration. At the same time, using a Fourier spectral method to approximate spatial derivatives gives much higher accuracy than finite difference methods [27]. Thus, the use of a semi-implicit Fourier spectral method enabled us to integrate Eq. (5) for long times and large system sizes. The general idea behind the semi-implicit Fourier method is as follows. Consider the partial differential equation

$$\frac{\partial u(x, t)}{\partial t} = \hat{\mathbf{L}}u(x, t) + \hat{\mathbf{N}}[u(x, t), \partial_x u(x, t), \partial_x^2 u(x, t), \dots], \quad (12)$$

where $\hat{\mathbf{L}}$ is a linear differential operator and $\hat{\mathbf{N}}$ is a nonlinear functional of u and its spatial derivatives. If we discretize space into N (not to be confused with $\hat{\mathbf{N}}$) grid points with lattice spacing h and denote the value of the field $u(x, t)$ at each grid point by $u_i(t)$, we obtain a system of ordinary differential equations:

$$\frac{du_i}{dt} = (\hat{\mathbf{L}}u)_i + \hat{\mathbf{N}}[u(x, t), \dots]_i \quad i = 0, 1, \dots, N-1. \quad (13)$$

Taking the discrete Fourier transform of this equation gives

$$\frac{d\tilde{u}_k}{dt} = (\hat{\mathbf{L}}u)_k + \tilde{\mathbf{N}}_k \quad k = 0, 1, \dots, \frac{N}{2} - 1, -N/2, \dots, -1. \quad (14)$$

For the (deterministic) SKS equation,

$$\hat{\mathbf{L}}u(x, t) = -\alpha u(x, t) - \partial_x^2 u(x, t) - \partial_x^4 u(x, t) \quad (15)$$

and

$$\hat{\mathbf{N}}[u(x, t), \partial_x u(x, t)] = [\partial_x u(x, t)]^2 \quad (16)$$

The Fourier transform of the discretized field u_i can be found numerically using the fast Fourier transform (FFT). If \tilde{u}_k denotes the k th wave-number component of the discrete Fourier transform of the field u , then the discrete Fourier transform of Eq. (15) is [27]

$$(\hat{\mathbf{L}}u)_k = -\alpha \tilde{u}_k + (2\pi k/Nh)^2 \tilde{u}_k - (2\pi k/Nh)^4 \tilde{u}_k. \quad (17)$$

Evaluating the nonlinear term $\tilde{\mathbf{N}}_k[u(x, t), \dots]$ in Fourier space directly is computationally expensive, since the Fourier transform of a product of functions is a convolution involving $O(N^2)$ computations. Therefore, we perform the integration by evaluating the nonlinear term in position space and then transforming it back to Fourier space. Putting all this together, we get

$$\frac{d\tilde{u}_k}{dt} = -\alpha \tilde{u}_k + (2\pi k/Nh)^2 \tilde{u}_k - (2\pi k/Nh)^4 \tilde{u}_k + \tilde{\mathbf{N}}_k[u(x, t), \dots]. \quad (18)$$

To solve the issue of small time step, we use a semi-implicit integration scheme. We integrate forward in time by treating the linear terms implicitly and the nonlinear term explicitly [26]. Let u_k^j be the value of u_k at time t_j . Then we approximate the time derivative by $du_k^j/dt = \frac{u_k^{j+1} - u_k^j}{\Delta t}$, and Eq. (18) becomes

$$u_k^{j+1} = \frac{u_k^j + \Delta t \tilde{\mathbf{N}}_k^j}{1 - \Delta t \left[-\alpha + \left(\frac{2\pi k}{Nh} \right)^2 - \left(\frac{2\pi k}{Nh} \right)^4 \right]}. \quad (19)$$

With this semi-implicit scheme, it became possible to increase the time step by a factor of about 50 compared to that in an explicit time integration scheme, without causing instabilities and without loss of accuracy. This resulted in a significant speed up of the algorithm. Finally, in order to incorporate noise, we let ζ_k^j denote the value of the noise term at time t_j , and Eq. (19) is modified to read

$$u_k^{j+1} = \frac{u_k^j + \Delta t \tilde{\mathbf{N}}_k^j + \sqrt{\frac{2\varepsilon N \Delta t}{h}} \zeta_k^j}{1 - \Delta t \left[-\alpha + \left(\frac{2\pi k}{Nh} \right)^2 - \left(\frac{2\pi k}{Nh} \right)^4 \right]}, \quad (20)$$

where $\langle \zeta_k^j \rangle = 0$ and $\langle \zeta_k^j \zeta_{k'}^{j'} \rangle = \delta_{k, -k'} \delta_{j, j'}$. This is simply the Itô formula for the solution of a stochastic differential equation [28]. The procedure for generating noise in Fourier space which satisfies equations Eqs. (6) and (7) is also given in Ref. [28], Appendix B.

V. RESULTS

Our aim is to compute the empirical probability distribution for the allowed periodic states and determine if the distribution has a peak at a particular wave number. If such a peak is present, it would support the hypothesis that noise is a possible mechanism of wave-number selection. To do this,

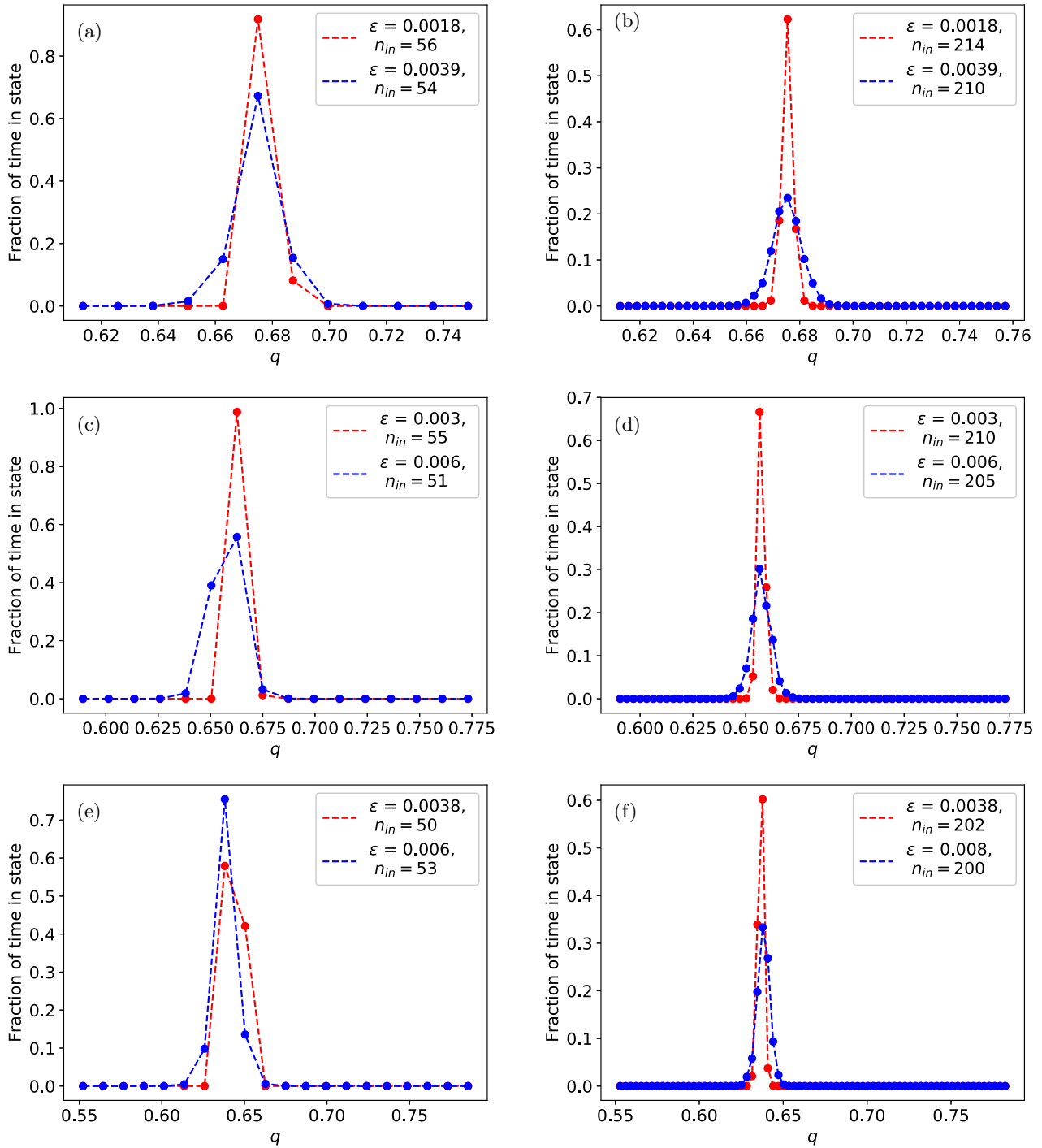


FIG. 2. Empirical probability distributions for various control parameter values and small and large system sizes. (a) $\alpha = 0.22, N = 1024$; (b) $\alpha = 0.22, N = 4000$; (c) $\alpha = 0.20, N = 1024$; (d) $\alpha = 0.20, N = 4000$; (e) $\alpha = 0.17, N = 1024$; (f) $\alpha = 0.17, N = 4000$.

we used noise strengths that are around 0.1% of the amplitude of the field $u(x, t)$. This noise strength is quite large, but it allowed the system to explore a large number of states. We started the simulation with the system initially placed in one of the periodic states and then perturbed it with noise. The noise caused the system to visit other steady states. We then counted the number of times each periodic state was visited and computed the fraction of the time spent in each state, for long runs of $\sim 10^8$ time steps. Our hypothesis was that the system would spend the greatest fraction of time in the

most stable or selected state. It is important to clarify what we mean by “visiting a given periodic state.” In the presence of large noise strengths, the state of the system at any given time has a broad power spectrum, with nonzero components for several wave numbers, and it is, strictly speaking, inaccurate to say that the system is in a given periodic state. Instead, we consider the system to be in the neighborhood of a periodic state, if the power spectrum has a peak at that periodicity, and if the Fourier component at that periodicity is at least twice as large as the other Fourier components. Hence, what

TABLE I. Most visited wave numbers for various sizes, $\alpha = 0.22$.

Number of lattice points N	System length ($L = Nh$)	Most visited state
1024	512	0.6749 ($n = 55$)
1600	800	0.6754 ($n = 86$)
2200	1100	0.6740 ($n = 118$)
3000	1500	0.6744 ($n = 161$)
4000	2000	0.6754 ($n = 215$)

we actually calculated was the empirical probability for being near a periodic state. To do so, we calculated the time average of the *indicator function* for a state with wave number q ,

$$M_T(q) = \frac{1}{T} \int_0^T \mathbf{1}_q(t) dt. \quad (21)$$

If the system is in a state with a power spectrum peaked at wave number k (and this peak is at least twice as large as other peaks), then the indicator function for wave number q is defined by

$$\mathbf{1}_q(t) = \begin{cases} 1 & k = q \text{ at time } t \\ 0 & \text{otherwise} \end{cases}. \quad (22)$$

This quantity gives the fraction of time spent near the state with wave number q and approaches the stationary probability distribution at very long times:

$$\lim_{T \rightarrow \infty} M_T(q) = P_{st}(q). \quad (23)$$

Since wave-number selection has already been demonstrated for a small system with control parameter $\alpha = 0.24$ in Ref. [11], we attempted to carry out the procedure described above for $\alpha = 0.22$. We restricted our simulations to the interval $0.16 < \alpha < 0.25$, since for $\alpha \leq 0.16$ the second harmonic in the stationary solution becomes active, in addition to the fundamental harmonic, leading to complicated instabilities [14]. For $\alpha = 0.22$, the wave numbers that are stable to perturbations lie within the range $0.6136 \leq q \leq 0.7486$, [14]. We used periodic boundary conditions, which implies that out of the wave numbers in the above range, only those appeared in the simulation that satisfy

$$q_n = \frac{2\pi n}{Nh}, \quad (24)$$

where n is an integer ($1 \leq n \leq N$). Thus, the imposition of periodic boundary conditions limited the allowed wave numbers to a discrete set given by Eq. (24), with n representing the number of cells in the solution. For all our simulations, the

TABLE II. Most visited wave numbers for various sizes, $\alpha = 0.20$.

Number of lattice points N	System length ($L = Nh$)	Most visited state
1024	512	0.6627 ($n = 54$)
1600	800	0.6597 ($n = 84$)
2200	1100	0.6569 ($n = 115$)
3000	1500	0.6576 ($n = 157$)
4000	2000	0.6566 ($n = 209$)

TABLE III. Most visited wave numbers for various sizes, $\alpha = 0.17$.

Number of lattice points N	System length ($L = Nh$)	Most visited state
1024	512	0.6381 ($n = 52$)
1600	800	0.6361 ($n = 81$)
2200	1100	0.6340 ($n = 111$)
3000	1500	0.6367 ($n = 152$)
4000	2000	0.6377 ($n = 203$)

initial condition was of the form $u_{in} \sim \sin(2\pi n_{in}x/Nh)$ with n_{in} being an integer. For the range $0.6136 \leq q \leq 0.7486$, and $N = 1024$, $h = 0.5$, we have $50 \leq n \leq 61$. Our time step was $\Delta t = 0.3$.

We first used a small noise strength $\varepsilon = 10^{-4}$ to determine which states were the most stable. We found that the states with $n = 54, 55, 56$ were all very stable and the system could not be knocked out of them with this noise strength. In order to determine which one of these three states was the most stable, we increased the noise strength gradually and found that at $\varepsilon = 1.8 \times 10^{-3}$, the $n = 54$ and $n = 56$ states became unstable, while the $n = 55$ ($q = 0.6749$) state persisted. When we plotted the fraction of time spent near each state, the resulting histogram developed a peak at this state. This peak persisted until the end of the integration (about 10^8 time steps), indicating that the system spent most of its time near that state. The histogram was also seen to become narrower with time, again indicating that the system spent most of its time close to the $n = 55$ state. We ran a few simulations at $\varepsilon = 1.9 \times 10^{-3}$ and $\varepsilon = 3.9 \times 10^{-3}$ and again observed that after spending some time around $n = 54$ or $n = 56$, the system transitioned to a neighborhood of the $n = 55$ state and spent the most amount of time there [see Fig. 2(a)]. In all three cases, the histogram became nearly stationary after around 10^8 time steps. The observation that the most visited state remains the same in spite of increasing the noise strength is promising evidence of the selection of a unique state by noise. The most visited state was also found to be independent of initial condition.

We repeated these simulations for the same value of α , i.e., $\alpha = 0.22$, but different system sizes and noise strengths. In each case, we observed that after initially visiting a narrow band of states, the system settled down close to one of them. This state was independent of the noise strength and initial conditions. The largest system size we tried was $N = 4000$ lattice points, which gives us the most precise estimate of the selected wave number [see Fig. 2(b)]. For this size, the

TABLE IV. Most visited wave numbers for various sizes, $\alpha = 0.24$.

Number of lattice points N	System length ($L = Nh$)	Most visited state
1024	512	0.6995 ($n = 57$)
1600	800	0.6990 ($n = 89$)
2200	1100	0.6969 ($n = 122$)
3000	1500	0.6953 ($n = 166$)
4000	2000	0.6974 ($n = 222$)

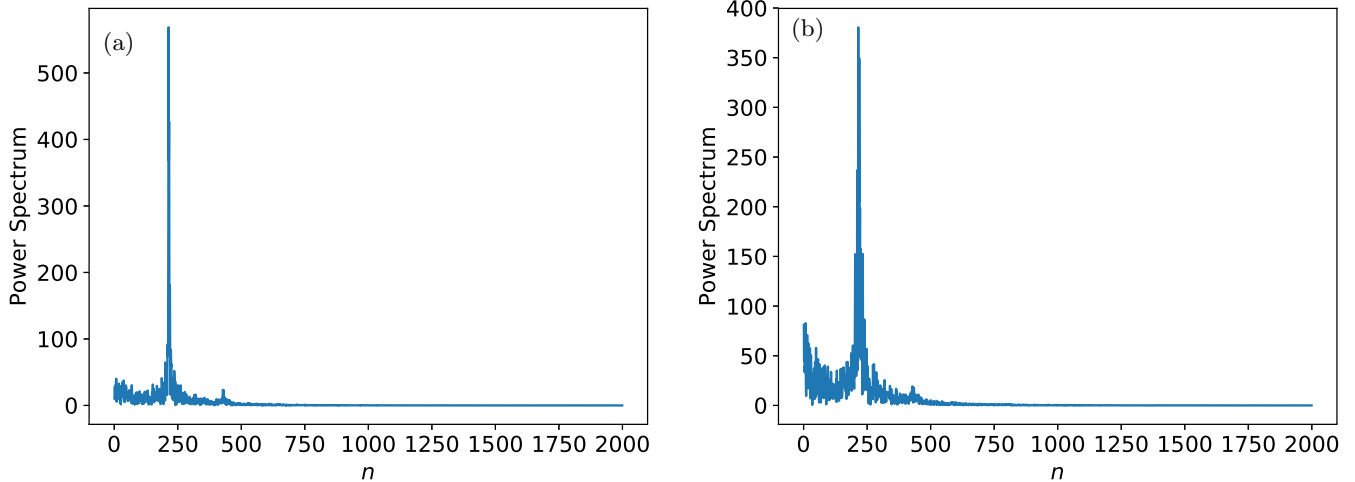


FIG. 3. Long-time power spectra for $\alpha = 0.22$ and 4000 lattice points. We have plotted the number of cells n in the solution on the x axis for visual clarity. (a) $\varepsilon = 0.0018$; (b) $\varepsilon = 0.0039$.

difference between two successive wave numbers is the smallest and is equal to $\Delta q = 2\pi/Nh = 0.003$. The most visited states for $\alpha = 0.22$ are presented in Table I. Thus, our best estimate for the selected wave number for $\alpha = 0.22$ is $q_s = 0.6754 \pm \Delta q/2$ or $q_s = 0.6754 \pm 0.0015$, corresponding to the case $N = 4000$.

Next, we repeated the same process for smaller values of α . As explained in Ref. [11], states in the middle of the Eckhaus band become more and more stable away from the threshold. This made it necessary to use slightly larger noise strengths to destabilize the states and obtain the required probability distributions. For $\alpha = 0.20$ and $N = 1024$, the Eckhaus stable wave numbers are $0.5890 \leq q \leq 0.7608$ or $48 \leq n \leq 62$. For a range of noise strengths between 3×10^{-3} and 6×10^{-3} and different initial conditions, we found $n = 54$ ($q = 0.6627$) to be the most visited state [Fig. 2(c)]. For $N = 4000$ lattice points, we found $n = 209$ to be the most visited state; see Fig. 2(d). Results for various system sizes are shown in Table II. Finally, results for $\alpha = 0.17$ are shown in Table III and Figs. 2(e) and 2(f).

Figure 2 shows that the width of the probability distributions shrinks as the system size increases and as the noise

strength decreases. However, the position of the maximum of the distributions remains unchanged. For the sake of completeness, we have also reproduced Obeid's result for $\alpha = 0.24$ and extended it to larger sizes, as shown in Table IV.

The power spectra at the end of integration for $\alpha = 0.22$ and low and high noise strengths are shown in Fig. 3. These figures show that the final power spectra have prominent maxima at the most visited wave number, in spite of the large noise strengths we have used. Small but visible second harmonic peaks are also observed, indicating that the system is close to a periodic steady state of the deterministic system. The power spectra for $\alpha = 0.20$ and 0.17 are similar. Note that we have plotted the number of cells n on the x axis, instead of the wave number.

We also show plots of the field $u(x, t)$ (for $\alpha = 0.22$ and 1024 lattice points) at very long times in Fig. 4. Figure 4(a) corresponds to $\varepsilon = 0.0018$, while Fig. 4(b) is for $\varepsilon = 0.0039$. Finally, a plot of the selected wave numbers for 4000 lattice points against α is shown in Fig. 5, with error bars representing the discretization error. It also shows the results obtained in Ref. [15] for the same values of α . Both curves show that as the value of α is decreased below the threshold, the selected

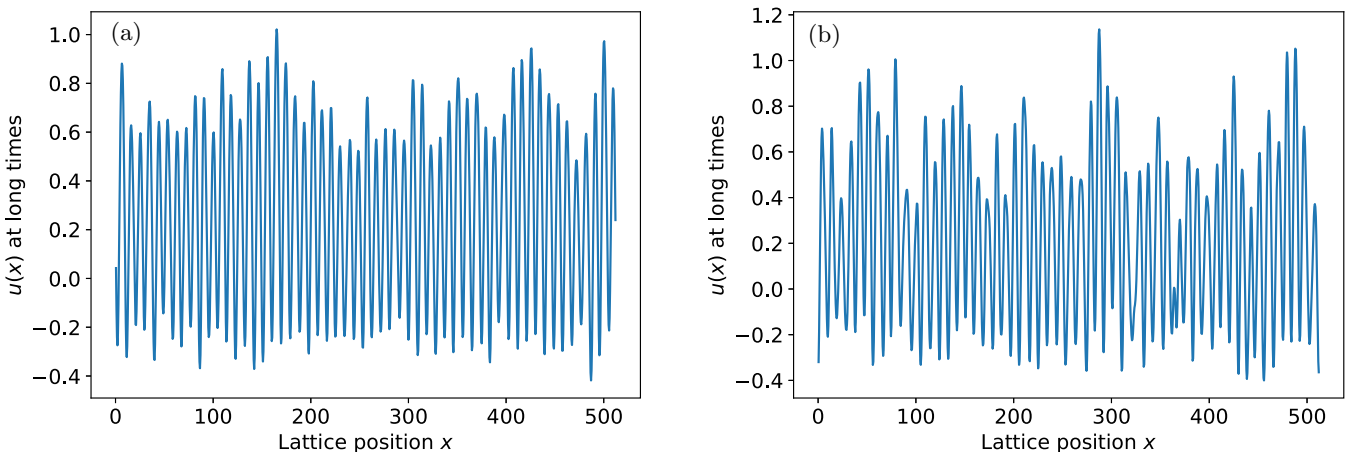


FIG. 4. Typical final configurations at the end of integration for $\alpha = 0.22$, 1024 lattice points. (a) $\varepsilon = 0.0018$; (b) $\varepsilon = 0.0039$.

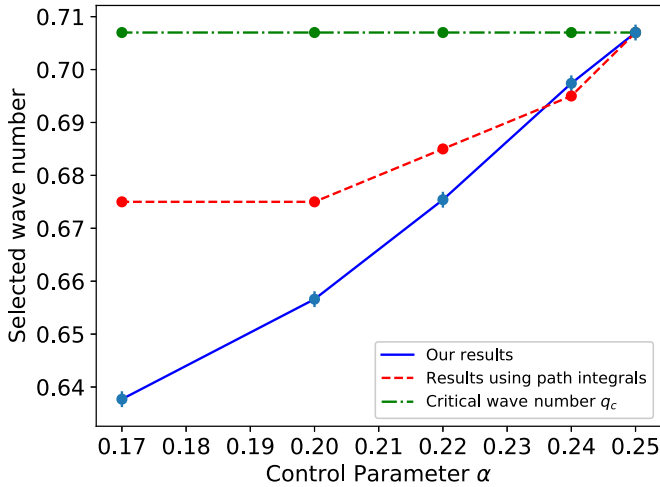


FIG. 5. Comparison of our results with those of Ref. [15]. The horizontal line represents the critical wave number $q_c = \frac{1}{\sqrt{2}}$, which is the fastest growing wave number in the linear stability analysis.

wave number is shifted to the left of the critical wave number q_c (horizontal line in Fig. 5). However, our values for the selected wave number do not agree with theirs far from $\alpha = \alpha_c$. We believe that the reason for the disagreement is likely numerical. Since the disagreement is particularly large away from the threshold, it is our view that the use of the amplitude equation may be inappropriate. It is possible, for example, that the saddle solution for the amplitude equation is not a sufficiently accurate initial guess for the true saddle state for α values far from 0.25. Second, the time-reversed deterministic path is the minimum action path only for potential systems [15]. While it is reasonable to assume that it would be a good initial guess for nonpotential systems, it is also possible that the actual minimum action path is far more complicated away from the threshold, where the nonpotential term in Eq. (5) is not small. The discretized action is a function of the discretized field at all lattice points and all times and hence could be an extremely complicated function, with possibly multiple

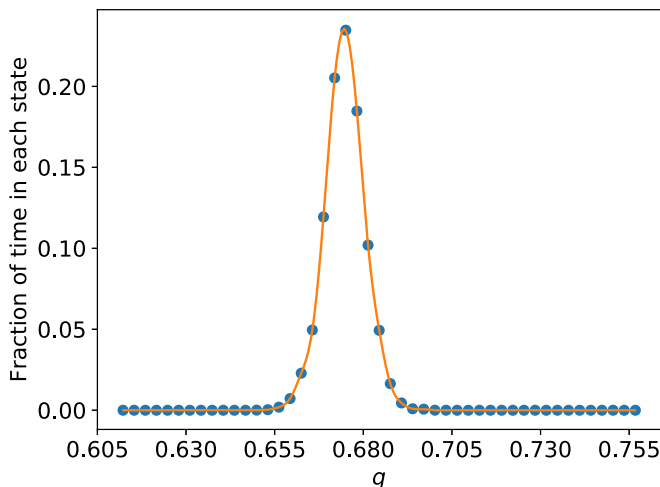


FIG. 6. Interpolating curve for $\alpha = 0.22$, with a maximum at $q_s = 0.6748$.

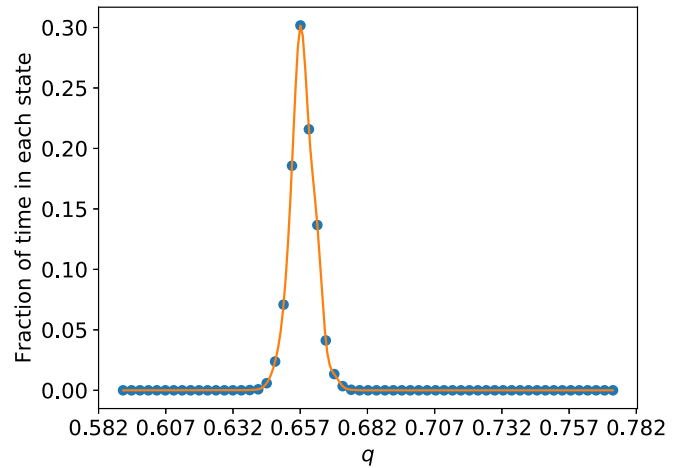


FIG. 7. Interpolating curve for $\alpha = 0.20$, with a maximum at $q_s = 0.6567$.

minima. It is not clear what kind of numerical uncertainties arise in minimizing this action, and whether the minimum action paths found in Ref. [15] are local minima or global minima. A thorough analysis of the optimization techniques is needed to explore these issues.

Extension to thermodynamic limit

It is interesting to note that the probability distributions we have obtained sharpen about the selected wave number as the system size is increased. This appears to be surprising, because the number of accessible wave numbers increases with system size, and hence, one would expect the histograms of Fig. 2 to become wider when the system size is increased. The emergence of new modes is, in fact, seen in Figs. 2(b), 2(d), and 2(f). However, the crucial observation is that these newly excited wave numbers lie in a narrower band than the excited wave numbers for a smaller system. Combined with the observation that the histograms and power spectra become broader with increasing noise strength, our findings are consistent with the existence of a correlation length ξ which diverges in the limit $\varepsilon \rightarrow 0$ and $N \rightarrow \infty$, but is finite

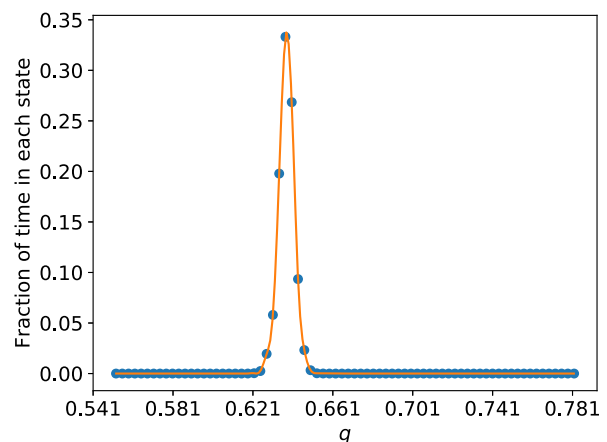


FIG. 8. Interpolating curve for $\alpha = 0.17$ with a maximum at $q_s = 0.6384$.

TABLE V. Most visited or selected wave numbers q_s in the thermodynamic limit.

Control Parameter α	q_s
0.22	0.6748
0.20	0.6567
0.17	0.6384

for finite ε and N . We emphasize that, at present, we cannot prove this assertion, but its validity is consistent with our data.

Assuming that the above claim is valid, one can use the discrete probability distributions obtained for finite system sizes to estimate the selected wave number for an infinite system (for which there exists a continuous band of allowed wave numbers). This is similar to the finite size scaling procedure in critical phenomena. We carried out this procedure using the histograms obtained for the largest system size, i.e., 4000 lattice points. To do so, we used cubic spline interpolation to get a smooth function passing through the discrete points obtained from our simulations. The continuous curves thus obtained show which wave number would be most probable in the continuum case. The results are shown in Figs. 6, 7, and 8. Our continuum estimates for the selected wave numbers are given in Table V.

We emphasize again that there is no scaling theory for systems such as the one we have studied, so that the existence of a divergent correlation length cannot be conclusively proved at present. Finally, we note that there is another explanation for the sharpening of the probability distributions with increasing system size: namely, that there is a *finite* correlation length, but this length is greater than the largest system size we have used (for the noise strengths used in our simulations). This is certainly possible for the lower end of the noise strengths we have used. However, we believe that this is unlikely to be the case for the higher end of noise strengths. The power spectrum in Fig. 3(b) is quite broad (in spite of having a prominent peak at the selected wave number), which implies that the correlation length is smaller than the system size.

VI. CONCLUSIONS

We have performed a detailed numerical study of noise-induced wave number selection in the one dimensional SKS

equation. We have shown that even in the presence of large noise, long-time power spectra of the field are most likely to be peaked at a unique wave number that does not depend on the initial state or the noise strength. We note again that due to the large noise strengths we had to use, there were nonzero Fourier components at other wave numbers, which means that for finite system sizes and large noise strengths, there is no true selection, as expected. However, since the position of the peak of the power spectrum was found to be independent of noise strength and since the probability distributions were seen to become sharper with increasing system size and decreasing noise strength, it is plausible to conclude that the same wave number would be selected for noise strengths much less than the ones used here, except that it would require prohibitively large integration times.

It is interesting to compare our findings with other selection mechanisms proposed in Refs. [5–7]. As discussed there, control parameter ramps are an efficient way to select a unique, well-defined wave number. However, Ref. [7] also shows that varying different quantities that lead to the same final control parameter results in different selected wave numbers. Reference [4] has shown that starting from random initial conditions and simulating deterministically, the final wave number depends on the initial state. In contrast, our work shows that at long times, the system is most likely to be found in a state with a dominant wave number, and this dominant wave number does not depend on initial conditions or noise strength, but is an intrinsic property of the SKS system. We have been able to show this for a wide range of control parameters and large system sizes, in contrast to previous work. Our work shows that noise-induced wave-number selection can occur in nonpotential systems. Much remains to be done however; a future direction could be to devise efficient importance sampling techniques which would enable us to study transitions between states without using large noise strengths. It would also be interesting to see if it is possible to predict the selected wave number analytically, although to our knowledge no such analytical theory exists.

ACKNOWLEDGMENTS

S.S. thanks Dr. Ken Elder for useful discussions about the simulation algorithm.

-
- [1] M. C. Cross and P. C. Hohenberg, *Rev. Mod. Phys.* **65**, 851 (1993).
 - [2] B. Grossmann, K. R. Elder, M. Grant, and J. M. Kosterlitz, *Phys. Rev. Lett.* **71**, 3323 (1993).
 - [3] M. C. Cross and H. Greenside, *Pattern Formation and Dynamics in Nonequilibrium Systems* (Cambridge University Press, New York, 2009).
 - [4] H. R. Schober, E. Allroth, K. Schroeder, and H. Müller-Krumbhaar, *Phys. Rev. A* **33**, 567 (1986).
 - [5] D. S. Cannell, M. A. Dominguez-Lerma, and G. Ahlers, *Phys. Rev. Lett.* **50**, 1365 (1983).
 - [6] L. Kramer, E. Ben-Jacob, H. Brand, and M. C. Cross, *Phys. Rev. Lett.* **49**, 1891 (1982).
 - [7] P. C. Hohenberg, L. Kramer, and H. Riecke, *Physica D* **15**, 402 (1985).
 - [8] M. Kerszberg, *Phys. Rev. B* **27**, 3909 (1983).
 - [9] M. Kerszberg, *Phys. Rev. B* **28**, 247 (1983).
 - [10] R. N. C. Filho, J. M. Kosterlitz, and E. Granato, *Physica A* **354**, 333 (2005).
 - [11] D. Obeid, J. M. Kosterlitz, and B. Sandstede, *Phys. Rev. E* **81**, 066205 (2010).
 - [12] J. Viñals, E. Hernández-García, M. San Miguel, and R. Toral, *Phys. Rev. A* **44**, 1123 (1991).
 - [13] J. Swift and P. C. Hohenberg, *Phys. Rev. A* **15**, 319 (1977).
 - [14] C. Misbah and A. Valance, *Phys. Rev. E* **49**, 166 (1994).

- [15] L. Qiao, Z. Zheng, and M. C. Cross, *Phys. Rev. E* **93**, 042204 (2016).
- [16] I. Bena, C. Misbah, and A. Valance, *Phys. Rev. B* **47**, 7408 (1993).
- [17] J. García-Ojalvo, A. Hernández-Machado, and J. M. Sancho, *Phys. Rev. Lett.* **71**, 1542 (1993).
- [18] J. M. R. Parrondo, C. V. den Broeck, J. Buceta, and J. de la Rubia, *Physica A* **224**, 153 (1996).
- [19] D. A. Kurtze, *Phys. Rev. Lett.* **77**, 63 (1996).
- [20] H. Risken, *The Fokker-Planck Equation: Methods of Solution and Applications* (Springer-Verlag, Berlin, 1989).
- [21] H. S. Greenside and M. C. Cross, *Phys. Rev. A* **31**, 2492 (1985).
- [22] E. Hernández-García, J. Viñals, R. Toral, and M. San Miguel, *Phys. Rev. Lett.* **70**, 3576 (1993).
- [23] E. Hernández-García, M. San Miguel, R. Toral, and J. Viñals, *Physica D* **61**, 159 (1992).
- [24] M. I. Freidlin and A. D. Wentzell, *Random Perturbations of Dynamical Systems* (Springer, New York, 2012).
- [25] L. Kramer and W. Zimmermann, *Physica D* **16**, 221 (1985).
- [26] L. Q. Chen and J. Shen, *Comput. Phys. Commun.* **108**, 147 (1998).
- [27] L. N. Trefethen, *Spectral Methods in MATLAB* (SIAM, Philadelphia, 2000).
- [28] J. Garcia-Ojalvo and J. M. Sancho, *Noise in Spatially Extended Systems* (Springer-Verlag, New York, 1999).